ARMY RESEARCH LABORATORY

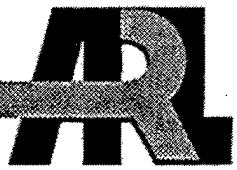

Optimizing a Slingatron Launcher Using MATLAB

by Mark L. Bundy, Gene R. Cooper,
and Stephen A. Wilkerson

ARL-TR-2555 August 2001

The findings in this report are not to be construed as an official Department of the Army position unless so designated by other authorized documents.

Citation of manufacturer's or trade names does not constitute an official endorsement or approval of the use thereof.

Destroy this report when it is no longer needed. Do not return it to the originator.

Army Research Laboratory
Aberdeen Proving Ground, MD 21005-5066

ARL-TR-2555 **August 2001**

Optimizing a Slingatron Launcher Using MATLAB

Mark L. Bundy, Gene R. Cooper, and Stephen A. Wilkerson
Weapons and Materials Research Directorate, ARL

Abstract

A slingatron is the name given to a propellantless mechanical means of launching a projectile. To date, slingatrons are only conceptual in nature, but their potential use as a ground-to-space launch mechanism for unmanned payloads is under investigation. Slingatrons can be configured in a variety of geometries; one form consists of a spiral track (or launch tube) that gyrates at a constant frequency about a set radius. Under proper conditions (design parameters), a projectile entering the spiral at its small radius end will undergo nearly constant tangential acceleration before exiting. The differential equations governing the motion of the projectile with the spiral are highly nonlinear, making the optimum design solution nonintuitive. This report describes how the slingatron works, from first principles, then uses the numerical integration procedures within the computer software environment of Simulink and MATLAB to search for and identify the optimum design solution parameters based on structural dynamics and mechanical design considerations.

REPORT DOCUMENTATION PAGE

Form Approved
OMB No. 0704-0188

1. AGENCY USE ONLY *(Leave blank)*	2. REPORT DATE	3. REPORT TYPE AND DATES COVERED
	August 2001	Final, August 2000–January 2001

4. TITLE AND SUBTITLE
Optimizing a Slingatron Launcher Using MATLAB

5. FUNDING NUMBERS
1L162618AH80

6. AUTHOR(S)
Mark L. Bundy, Gene R. Cooper, and Stephen A. Wilkerson

7. PERFORMING ORGANIZATION NAME(S) AND ADDRESS(ES)
U.S. Army Research Laboratory
ATTN: AMSRL-WM-BC
Aberdeen Proving Ground, MD 21005-5066

8. PERFORMING ORGANIZATION REPORT NUMBER
ARL-TR-2555

9. SPONSORING/MONITORING AGENCY NAMES(S) AND ADDRESS(ES)

10.SPONSORING/MONITORING AGENCY REPORT NUMBER

11. SUPPLEMENTARY NOTES

12a. DISTRIBUTION/AVAILABILITY STATEMENT
Approved for public release; distribution is unlimited.

12b. DISTRIBUTION CODE

13. ABSTRACT *(Maximum 200 words)*

A slingatron is the name given to a propellantless mechanical means of launching a projectile. To date, slingatrons are only conceptual in nature, but their potential use as a ground-to-space launch mechanism for unmanned payloads is under investigation. Slingatrons can be configured in a variety of geometries; one form consists of a spiral track (or launch tube) that gyrates at a constant frequency about a set radius. Under proper conditions (design parameters), a projectile entering the spiral at its small radius end will undergo nearly constant tangential acceleration before exiting. The differential equations governing the motion of the projectile with the spiral are highly nonlinear, making the optimum design solution nonintuitive. This report describes how the slingatron works, from first principles, then uses the numerical integration procedures within the computer software environment of Simulink and MATLAB to search for and identify the optimum design solution parameters based on structural dynamics and mechanical design considerations.

14. SUBJECT TERMS	15. NUMBER OF PAGES
slingatron, optimum, design, parameters, MATLAB, Simulink	39
	16. PRICE CODE

17. SECURITY CLASSIFICATION OF REPORT	18. SECURITY CLASSIFICATION OF THIS PAGE	19. SECURITY CLASSIFICATION OF ABSTRACT	20. LIMITATION OF ABSTRACT
UNCLASSIFIED	UNCLASSIFIED	UNCLASSIFIED	UL

INTENTIONALLY LEFT BLANK.

Table of Contents

INTENTIONALLY LEFT BLANK.

List of Figures

List of Tables

INTENTIONALLY LEFT BLANK.

1. Purpose of This Study

The cost of launching payloads into space is currently $10,000 per pound. Although this expense may be acceptable for manned space missions, it can be a curtailing financial burden for other potential enterprises. Less expensive alternative methods of launching gravity-insensitive bulk items into space is thus an area of interest. The slingatron is a proposed propellantless means of space launching such objects (Tidman et al. 1995, Tidman 1996, Tidman 1998, Tidman and Greig 1999). This study describes the operational principles of the slingatron and investigates the range of possible design solutions using MATLAB and Simulink software, thus bounding the physical scale, if not the cost, of such a launch device.

2. The Operational Principles a Slingatron Launcher

Those who played with a Hula-Hoop as a child and remember how the sound of the ball's speed within the hoop increased with the gyration rate of the hips, might recognize the similarity with a projectile in a slingatron. Figures 1–3 show the progression of forces in action in going from uniform circular motion to circular slingatron (or, Hula-Hoop-type) motion. Specifically, Figure 1 displays uniform circular motion of a ball of mass m about a circle of radius D, with velocity $\vec{v}$ (of constant magnitude), due to a centripetal force $\vec{F}_D$ (of constant magnitude). The circular speed in this case is given by:

$$|\vec{v}| = \sqrt{\frac{D|\vec{F}_D|}{m}} \quad . \tag{1}$$

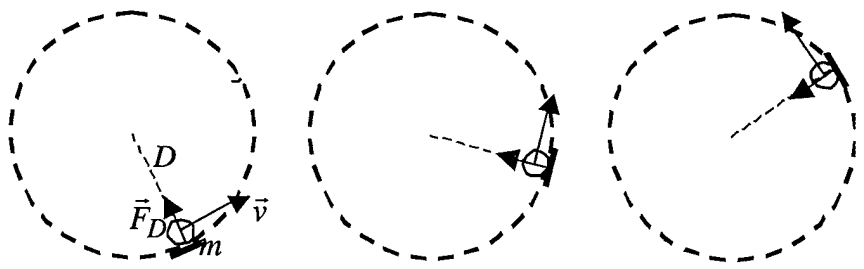

Figure 1. Uniform Circular Motion.

The speed of the ball in Figure 1 can be increased by orienting the normal force acting on the ball so that it has a tangential as well as a centripetal component. This could be done by envisioning a rotating wedge, as shown in Figure 2. As the circular speed of the ball increases under the tangential force, so too must the circular speed (angular velocity) of the supporting wedge. The normal force of the wedge on the ball must also increase (with an increase in angular velocity) in order to counterbalance the increasing centrifugal force of the ball on the wedge (hence $\bar{F}_\perp < \bar{F}_\perp' < \bar{F}_\perp''$ in Figure 2). More abstractly, it is possible to view the ball as riding on the up-slope of a wave rather than a wedge. The "buoyant" force and rotational frequency, or wave speed, must also increase to keep (supporting) pace with the increasing speed of the ball. From either perspective, the time rate of change of the object's speed would be given by:

$$\frac{d|\vec{v}|}{dt} = \frac{|\vec{F}_\perp|\sin\gamma}{m} = \frac{|\vec{v}|^2 \tan\gamma}{D} \quad . \tag{2}$$

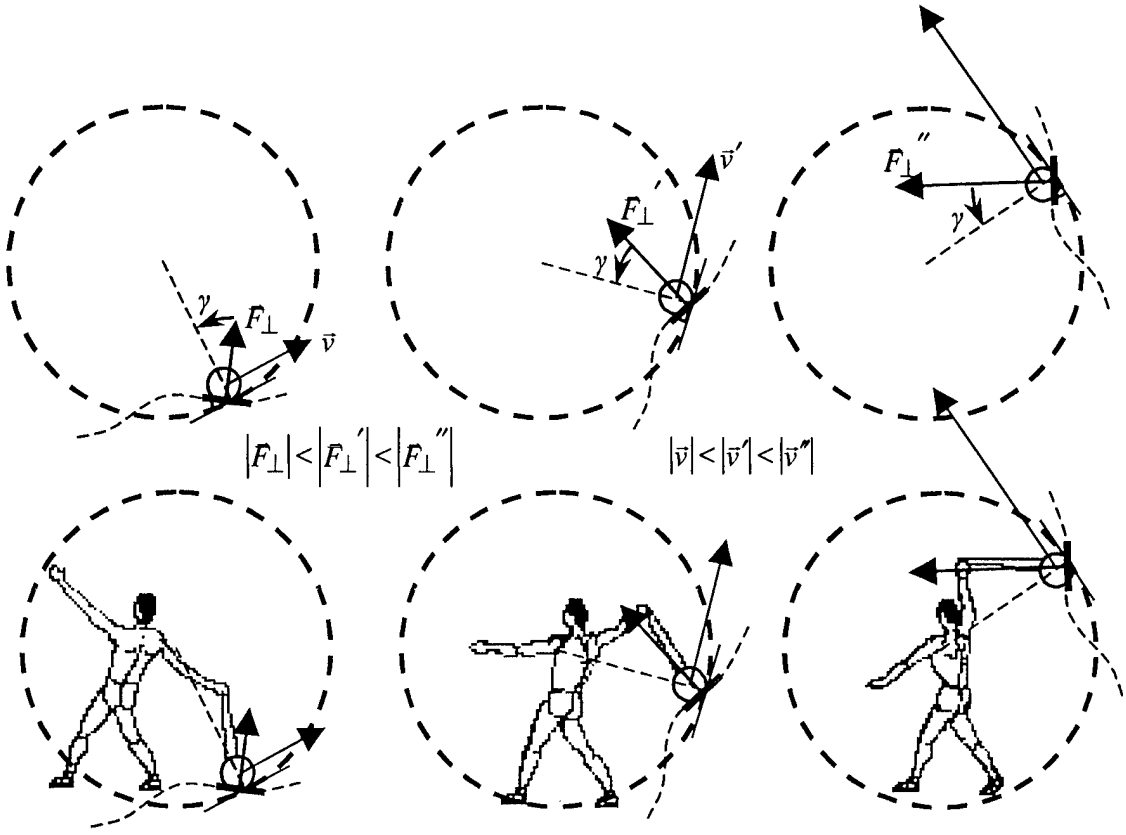

Figure 2. Nonuniform Circular Motion Created by the Tangential Force Component of a Rotating Wedge, Wave, or Sling.

Note, if γ is positive in Equation 2 and Figure 2, the speed will increase; whereas, if γ is negative, it decreases. When $\gamma = 0$, the speed stays constant (equivalent to Equation 1, Figure 1).

The effect of the rotating wedge (or wave) on mass m in Figure 2 can be duplicated by employing a gyrating ring of radius R, and therein lies the operational principle of the circular slingatron (or Hula-Hoop), as shown in Figure 3. As indicted in the illustration, the gyrating ring can provide the same boundary geometry and normal force as the wedge. Like the wedge, the frequency of gyration, $\dot{\psi}$, must increase for the ring to maintain its support for and stay in phase with the object.

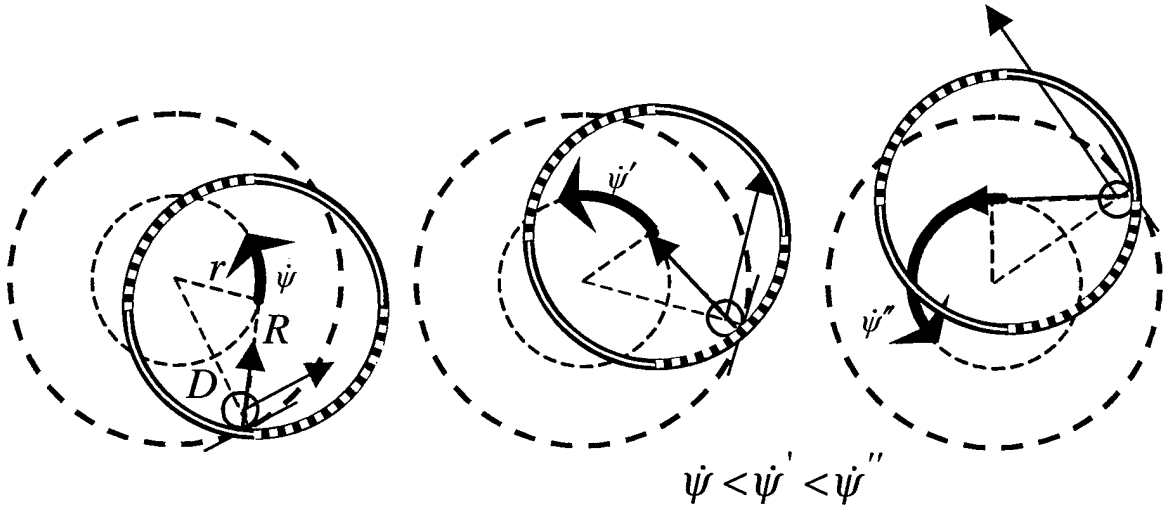

Figure 3. Nonuniform Circular Motion Created by a Gyrating Ring.

In addition to the Hula-Hoop, Figure 4(a), swirling liquid in a cup by moving the hand in a circular pattern (oxidizing wine in glass, for instance, Figure 4[b]) is another practical example of the same effect. In this case, the wave in the fluid moves up and around the sides of the cup/glass, with the wave amplitude of the liquid staying constant unless the gyration frequency of the hand/cup is increased. (As a practical exercise, hand swirling liquid in a cup reveals how important the phase angle is to maintaining, or increasing, the wave speed/amplitude.)

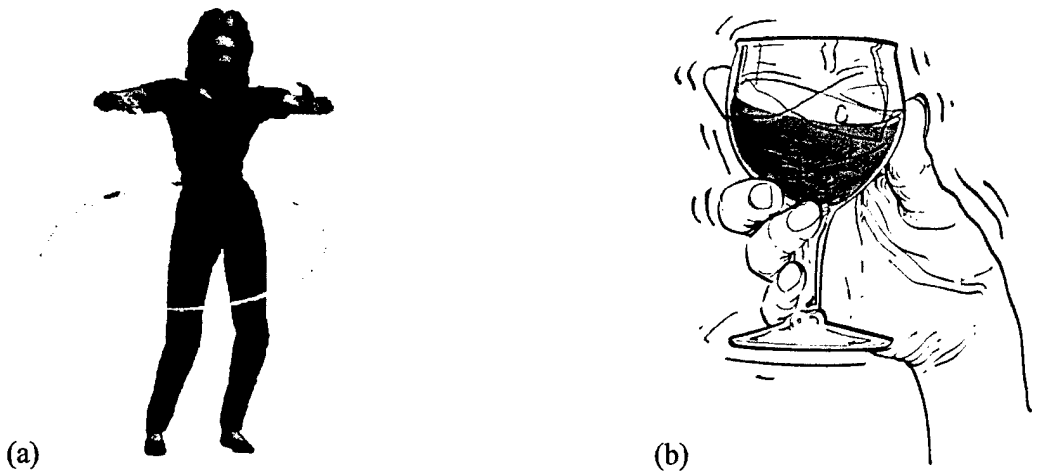

Figure 4. Slingatron-Like Motion Observed in the Action of (a) a Hula Hoop or (b) Swirling Liquid in a Glass.

Unlike the wedge (or ancient sling) in Figure 2, which rotates with the object (i.e., with no relative motion between the two), the ball in Figure 3 must execute circular motion within the gyrating ring. This relative motion can be detected in the illustration by observing that the ball is in contact with different zones (shaded arc lengths) along the gyrating ring's boundary as it moves about its circular path of radius D. Figure 5 shows the general orientation of the normal and tangential (frictional) force on the object, as well as specifying a set of reference angles. It can be said that the ring radius, R, lags the gyration radius, r, by the phase angle $\theta\,(=\psi - \varphi)$.

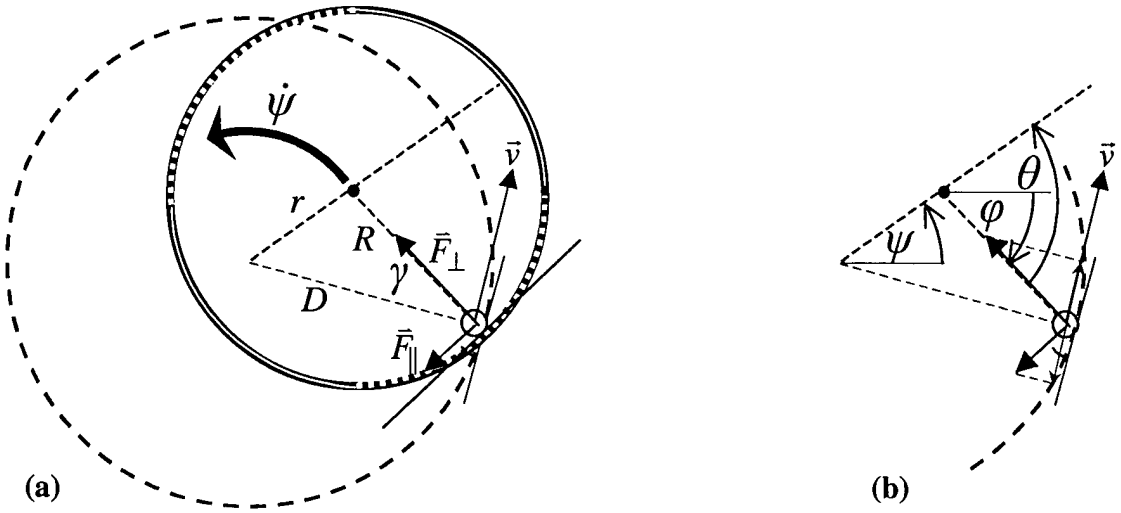

Figure 5. Normal and Frictional Force (a) of the Gyrating Ring on the Circulating Mass, With (b) Tangential Components That Affect the Object's Speed.

Thus far, the discussion has been limited to a circular slingatron track. However, such a configuration poses the practical problem of designing a mechanical gate to release the projectile after it reaches the sought after speed, e.g., earth-to-space "escape" velocity. For this reason, an open-ended spiral slingatron is a more feasible projectile-launching track geometry.

Making the conceptual transition from a circular to a spiral slingatron is facilitated by viewing a particular type of spiral that is composed of interconnected semicircular arc lengths, as shown in Figure 6(a). At any given time and location, the track is moving within a gyrating circular arc, as it was in Figure 5. Here, however, the radius of the circular arc changes every half-revolution, so that an object moving within the track must cover an ever increasing arc length (i.e., it must accelerate) in order to complete one revolution in phase with gyrating track, Figure 6(b). Thus, it is conceivable that under the right force conditions (normal track and friction force values) the object can continuously accelerate, even if the period of gyration stays the same.

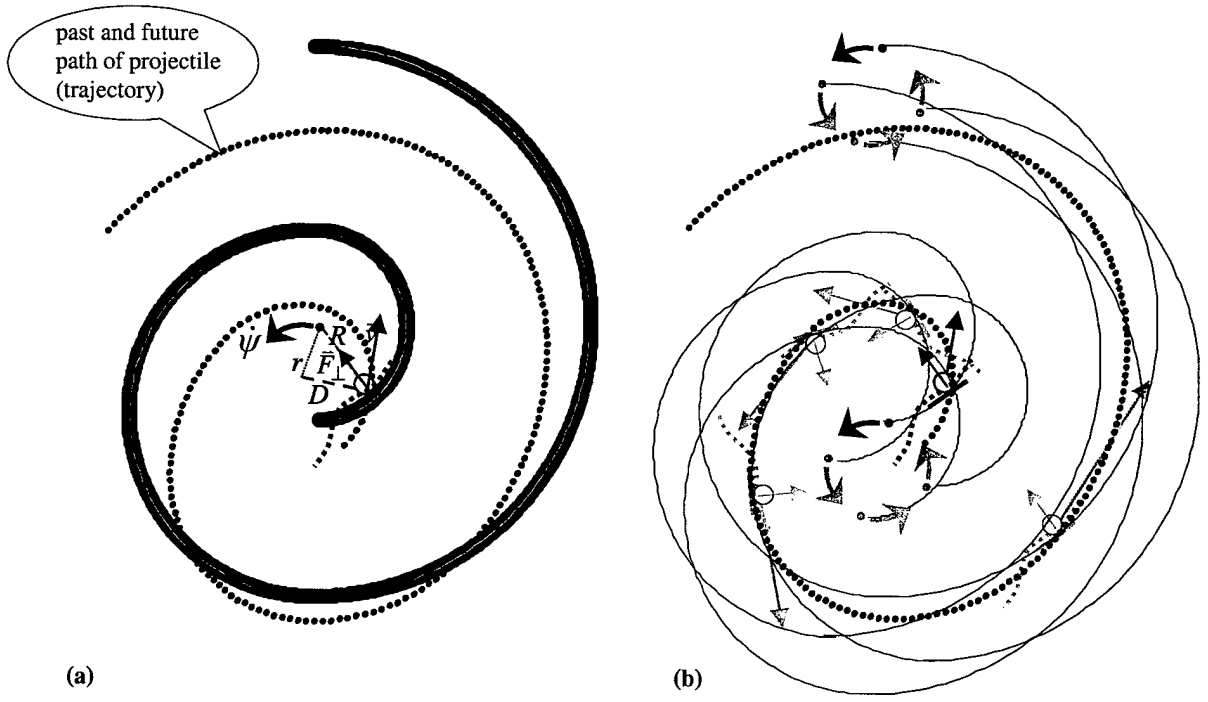

Figure 6. Spiral Slingatron, (a) Initial and (b) First Four Quarter-Cycle Gyration Conditions.

3. Equation of Motion for a Slingatron

The trajectory of the object in Figure 6 is redrawn in Figure 7, with the track and the object in motion suppressed to facilitate visualization of the object's velocity, force, and angular orientation. Unlike the gyrating ring of Figure 5, where the normal force was always directed toward the center of the ring, the direction of the normal force in the gyrating spiral depends on the spiral geometry, $R = R(\phi)$. It can also be characterized by the angle β (Figure 7), defined in Equation 3. Note that if R does not change with time (or ϕ), the spiral is actually a circle and $\beta = 0$.

$$\beta = \tan^{-1}\left(\frac{\dot{R}}{R\dot{\phi}}\right) = \tan^{-1}\left(\frac{1}{R}\frac{dR}{d\varphi}\right) \quad . \tag{3}$$

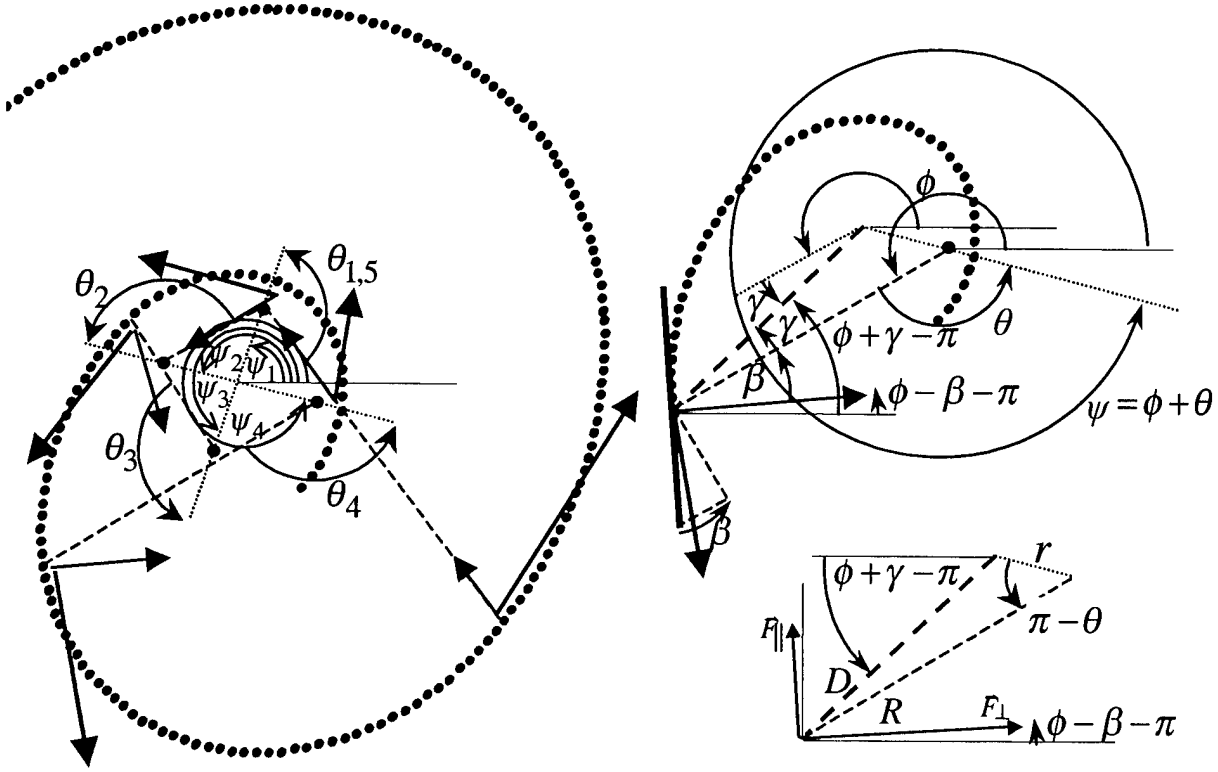

Figure 7. Kinematics of a Spiral Slingatron Trajectory.

Aided by Figure 7, the x- and y-components of Newton's second law of motion for an object of mass m in the spiral slingatron are:

$$\begin{aligned} m\ddot{x} &= \left|\vec{F}_{\perp}\right|\cos\{\phi-\beta-\pi\}-\left|\vec{F}_{\parallel}\right|\sin\{\phi-\beta-\pi\} \\ &= \left|\vec{F}_{\parallel}\right|\sin\{\phi-\beta\}-\left|\vec{F}_{\perp}\right|\cos\{\phi-\beta\} \\ m\ddot{y} &= \left|\vec{F}_{\perp}\right|\sin\{\phi-\beta-\pi\}+\left|\vec{F}_{\parallel}\right|\cos\{\phi-\beta-\pi\} \\ &= -\left|\vec{F}_{\perp}\right|\sin\{\phi-\beta\}-\left|\vec{F}_{\parallel}\right|\cos\{\phi-\beta\} \end{aligned} \tag{4}$$

In general, the force parallel to the track is due not only to track friction, but also to air friction/drag; therefore, assume that

$$\left|\vec{F}_{\parallel}\right| = \mu\left|\vec{F}_{\perp}\right| + PA \quad , \tag{5}$$

where μ is the coefficient of friction between the circulating mass (ball) and the gyrating track, P is the average frontal air pressure, and A is the object's frontal cross-sectional area. Using Equation 5 in Equation 4 yields

$$m\ddot{x}\left(\sin\{\phi-\beta\}+\mu\cos\{\phi-\beta\}\right)+m\ddot{y}\left(\mu\sin\{\phi-\beta\}-\cos\{\phi-\beta\}\right)=PA \quad . \tag{6}$$

Furthermore, in keeping with the geometry designations of Figure 7, the x and y components of the objects location can be written as

$$\begin{aligned} x &= r\cos\{\psi\}+R\cos\{\phi\} \\ y &= r\sin\{\psi\}+R\sin\{\phi\} \end{aligned} \tag{7}$$

Bearing in mind that r is constant and $R = R(\phi)$,

$$\ddot{x} = \ddot{\phi}\left[\frac{dR}{d\phi}\cos\phi - R\sin\phi\right] + \dot{\phi}^2\left[\frac{d^2R}{d\phi^2}\cos\phi - 2\frac{dR}{d\phi}\sin\phi - R\cos\phi\right]$$

$$-\ddot{\psi}\left[r\sin\psi\right] - \dot{\psi}^2\left[r\cos\psi\right]$$

$$\ddot{y} = \ddot{\phi}\left[\frac{dR}{d\phi}\sin\phi + R\cos\phi\right] + \dot{\phi}^2\left[\frac{d^2R}{d\phi^2}\sin\phi + 2\frac{dR}{d\phi}\cos\phi - R\sin\phi\right] \qquad (8)$$

$$+\ddot{\psi}\left[r\cos\psi\right] - \dot{\psi}^2\left[r\sin\psi\right]$$

Combining Equation 8 and Equation 6 yields the equation of motion for the spiral slingatron, viz.,*

$$R\ddot{\phi}\left[\tan\beta(\mu\cos\beta - \sin\beta) - (\cos\beta + \mu\sin\beta)\right]$$

$$+R\dot{\phi}^2\left[\left(\frac{d\tan\beta}{d\phi} + \tan^2\beta - 1\right)(\mu\cos\beta - \sin\beta) - 2\tan\beta\,(\cos\beta + \mu\sin\beta)\right]$$

$$+r\ddot{\psi}\begin{bmatrix}\sin\beta\{\sin(\psi-\phi) - \mu\cos(\psi-\phi)\} \\ -\cos\beta\{\cos(\psi-\phi) + \mu\sin(\psi-\phi)\}\end{bmatrix}$$

$$+r\dot{\psi}^2\begin{bmatrix}\cos\beta\{\sin(\psi-\phi) - \mu\cos(\psi-\phi)\} \\ +\sin\beta\{\cos(\psi-\phi) + \mu\sin(\psi-\phi)\}\end{bmatrix}$$

$$-\frac{PA}{m} = 0 \qquad , \qquad (9)$$

with β given by Equation 3. Note, if the spiral collapses into a circle, then $\beta = 0$, and the equation of motion for a circular slingatron becomes,

* With the exception of the pressure term, Eq. 9 agrees with the equation of projectile motion for a gyrating and evacuated spiral launch tube as derived by D. A. Tidman in his unpublished notes, dated November 11, 1997.

$$\ddot{\phi}R + \dot{\phi}^2\mu R + r\ddot{\psi}[\cos(\psi-\phi)+\mu\sin(\psi-\phi)] - r\dot{\psi}^2[\sin(\psi-\phi)-\mu\cos(\psi-\phi)] + \frac{PA}{m} = 0 \quad . \quad (10)$$

In this investigation, the only solutions of interest are those for which the gyration rate is steady, i.e., $\dot{\psi}$ is constant. (It is envisioned that the size of the spiral slingatron required for earth-to-space launch will be so massive that it would be difficult to provide such a large structure with any substantial angular acceleration over the short time period that the projectile traverses the launch tube.) Looking for solutions with $\ddot{\psi}=0$ means that the motion of an object in the spiral slingatron will conform to

$$\begin{aligned}
&R\ddot{\phi}\left[\tan\beta(\mu\cos\beta-\sin\beta) - (\cos\beta+\mu\sin\beta)\right] \\
&+R\dot{\phi}^2\left[\left(\frac{d\tan\beta}{d\phi}+\tan^2\beta-1\right)(\mu\cos\beta-\sin\beta) - 2\tan\beta\,(\cos\beta+\mu\sin\beta)\right] \\
&+r\dot{\psi}^2\begin{bmatrix}\cos\beta\left\langle\{\sin(\psi-\phi)-\mu\cos(\psi-\phi)\}\equiv\{\sin(\theta)-\mu\cos(\theta)\}\right\rangle \\ \\ +\sin\beta\left\langle\{\cos(\psi-\phi)+\mu\sin(\psi-\phi)\}\equiv\{\cos(\theta)+\mu\sin(\theta)\}\right\rangle\end{bmatrix} \quad . \quad (11) \\
&-\frac{PA}{m} = 0
\end{aligned}$$

Clearly, the differential equation describing the motion is nonlinear. A numerical solution is the only one possible. To this end, the numerical integration techniques within MATLAB (1998) and Simulink (both products of Mathworks Inc.) are used here to solve the problem. However, before invoking these solution algorithms, both μ and P need further clarification. For simplicity, a straightforward analytical expression* will be used for the average frontal pressure on the object in the slingatron, viz.,

* This expression can be derived from Equation 3.5, p. 64, of Liepman and Roshko (1957), in the limit of $P/P_\infty >> 1$ (i.e., high object/projectile velocity).

$$P = \frac{P_\infty \gamma(\gamma+1)M^2}{2} \quad , \tag{12}$$

where P_∞ is the gas pressure ahead of the object, γ is the ratio of specific heats, and M is the Mach number (defined as the ratio of the object's speed to that of the speed of sound in the gas ahead of the object). Furthermore, it is assumed here that air is in the launch tube ahead of the object, with $\gamma = 1.4$ and the speed of sound equal to 335 m/s. It was found that air drag can significantly retard the acceleration of the projectile in the slingatron unless the launch tube is partially evacuated. Since this study is primarily interested in finding the range of possible solutions, and evacuating a tube (even if it is a large tube) is not an insurmountable task, it was assumed from the outset that the launch tube could/would be pumped down to a pressure of $P_\infty = 0.01$ atm $= 1.01 \times 10^3$ N/m^2.

As for the friction coefficient, μ, this factor is also found to play a significant role in determining the size and speed of the slingatron needed to achieve the requisite earth-to-space escape velocity, assumed here to be 8 km/s. Tidman (2001) has obtained experimental data on μ for seeds up to 2 km/s. A curve fit to that data yielded the following simple expression:

$$\mu = \frac{0.12}{1.0 + 2.43 \times 10^{-3} \, |\vec{v}|} \quad . \tag{13}$$

For lack of a better alternative, i.e., until a broader range of data can be sampled, Equation 13 is utilized in Equation 11 to compute μ as a function of the object's velocity within the slingatron.

4. Solving the Equation of Motion

4.1 Simulink Formulation

Simulink offers a finite difference-based solution to ordinary differential equations. The user constructs the differential equation by linking together symbols (representative of mathematical subroutines) in a flowchart-like manner. For instance, assume the differential equation describing the vertical launch of a projectile into the atmosphere, subjected to aerodynamic drag and gravity forces, is given by

$$m\,\ddot{y} = F_{gravity} + F_{drag} = \frac{-G M_e\, m}{(R_{earth} + y)^2} + \frac{-C_D}{2}\left(\rho_0 e^{-y/5789}\right) A\,\dot{y}^2 \quad , \qquad (14)$$

where m is the mass of the projectile, y is the distance above the earth, G is the universal gravitational constant, M_e is the mass of the earth, R_{earth} is the radius of the earth, C_D is the drag coefficient, ρ_o is the density of air at the earth's surface, and A is the frontal cross-sectional area of the projectile. A Simulink flowchart representation of this differential equation is shown in Figure 8 (where a constant [high speed] drag coefficient of 0.1, a projectile of radius 0.3 m, an air density of 1.29 kg/m^3 at the earth surface, and projectile mass of 1000 kg are so-specified on their respective symbolic labels on the chart).

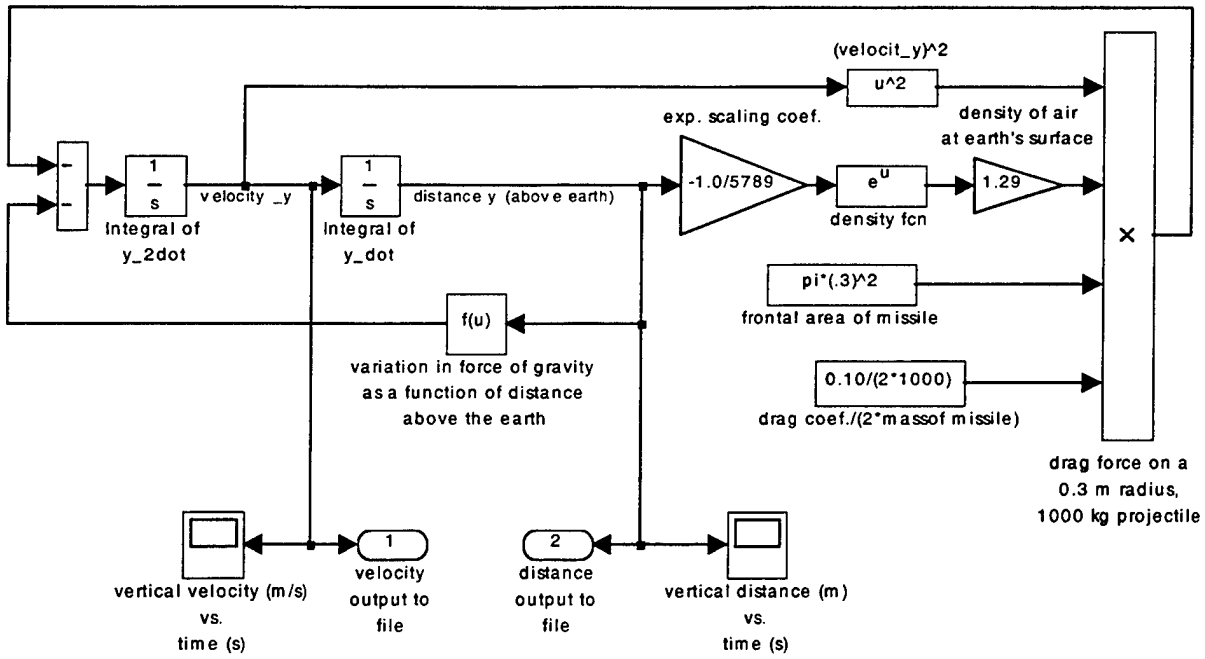

Figure 8. A Simulink Diagram of Equation 14.

Simulink has several options for viewing the numerical solution of the problem: one is pop-up windows (displayed as scope-like icons on the diagram in Figure 8), and another is to write the variables of interest to an output file (oval-like symbols in the diagram). Assuming an initial velocity of 8,000 m/s in the vertical direction, the Simulink solution of Equation 14 (and Figure 8) is shown plotted in Figure 9. As indicated, the vertical velocity drops off quickly (from 8,000 m/s to ~7,100 m/s) due to a substantial aerodynamic drag force, but the drag force diminishes rapidly with elevation because of the exponential decay in the air density. The results indicate that such a projectile would reach approximately 4,500 km (~2,800 mi) before it starts to return to earth (at ~1,500 s, or 25 min). (Most likely, a slingatron-based earth-to-space launch would be aimed at a nonvertical angle to give the trajectory an arc-like profile.)

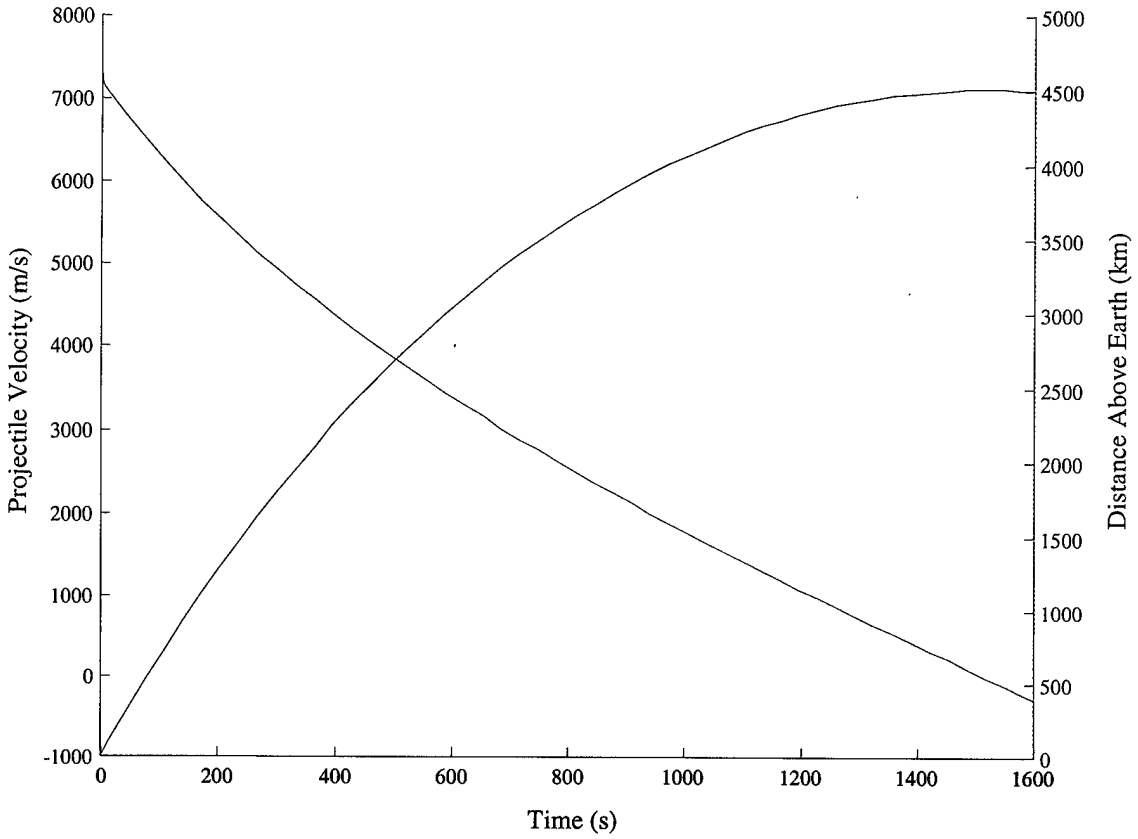

Figure 9. Simulink Solution of Equation (14), as Diagramed in Figure 8.

Having used Equation 14 and Figures 8 and 9 to illustrate the Simulink procedure for modeling and solving a simple nonlinear differential equation, Simulink was likewise used to solve the more complicated differential equation governing the motion of a spiral slingatron, specifically, Equation 11, as discussed next. (However, the Simulink flowchart representation of Equation 11 is not shown here; understandably, it is more detailed than the flowchart of Figure 8, representing Equation 14.)

4.2 Spiral Slingatron Parameters

Since $\dot{\psi}$ is the angular rate at which the spiral track gyrates, it is not a variable, but rather, a parameter of the problem. Likewise, the radius of gyration, r, is a parameter, as is the mass m and cross-sectional area A of the projectile. Depending on the geometry of the spiral, its description can involve several parameters; for instance, a circle requires one parameter—the radius. For simplicity, a two-parameter Archimedes spiral is assumed here, of the form

$$R(\phi) = a\,\phi + R_o \quad , \tag{15}$$

where a and R_o are two parameters. Initial conditions are also needed to specify the starting angles ψ_o and ϕ_o, as well as $\dot{\phi}_o$. Thus, there are a total of nine parameters that need to be specified to unambiguously solve Equation 11. However, not all of these parameters are varied in this exploratory investigation. In particular, ϕ_o is taken to be a constant, thereby defining a reference axis; also, the mass m is taken to be a constant, as is the projectile's cross-sectional area A. (The cross-sectional area is actually determined by specifying that the projectile has a certain fixed length-to-diameter ratio, and that it is composed of a fixed-mass outer steel shell containing a fixed-mass inner payload of water.) Furthermore, it is assumed that $\dot{\phi}_o$ is the same as $\dot{\psi}$, i.e., there is no initial time rate of change in the phase angle, θ. Hence, the number of parameters that will be varied in this report is reduced from nine to five.

4.3 Solution Results

Although a large range of solutions will ultimately be explored in this section, a small subset is chosen first to illustrate the solution routine and demonstrate that some of the parameters have more influence on the solution than others. With this in mind, the initial range of parameters is taken to be:

$$
\begin{aligned}
\dot{\psi} &= \frac{7\pi}{2}, \frac{9\pi}{2}, \frac{11\pi}{2} \text{ rad/s} \\
\dot{\phi}_o &= \dot{\psi} \\
\left.\begin{aligned} \psi_o &= \frac{\pi}{8}, \frac{\pi}{10}, \frac{\pi}{12} \text{ rad} \\ \phi_o &= 0 \text{ rad} \end{aligned}\right\} \theta_o &= \frac{\pi}{8}, \frac{\pi}{10}, \frac{\pi}{12} \text{ rad} \\
r &= 7.5, 9.5, 11.5 \text{ m} \\
R_o &= r+8,\ r+10,\ r+12 \text{ m} \\
a &= 0.175\times r,\ 0.225\times r,\ 0.275\times r \text{ m} \\
m &= 1{,}000 \text{ kg} \\
A &= 0.086 \text{ m}^2
\end{aligned}
\qquad (16)
$$

A command procedure was written, where the computed Simulink solution of Equation 11 (using Equations 3, 12, and 13, for β, P and μ, respectively) is obtained for each of the 243 combinations of parameters/initial conditions set out in Equation 16. A solution for $\phi(t)$ was considered acceptable for launching a projectile into space, if the computed value of the projectile's speed within the spiral track,

$$
\begin{aligned}
|\vec{v}| &= \sqrt{\dot{x}^2 + \dot{y}^2} \\
&= \dot{R}^2 + (r\dot{\psi})^2 + (R\dot{\phi})^2 + (2\dot{\psi}\,\dot{\phi}\,R\,r)\cos\theta - (2\dot{\psi}\;\dot{R}\,r)\sin\theta \qquad (17) \\
&= (\dot{\phi}\,a)^2 + (r\dot{\psi})^2 + ([a\phi + R_o]\dot{\phi})^2 + (2\dot{\psi}\,\dot{\phi}\,r\,[a\phi + R_o])\cos\theta - (2\dot{\psi}\,\dot{\phi}\,a\,r)\sin\theta
\end{aligned}
$$

reached 8 km/s at any time. Out of the 243 solutions, only 90 produced a projectile speed of at least 8 km/s. One such solution,

$$
\begin{aligned}
\dot{\psi} &= \frac{11\pi}{2} \text{ rad/s} \\
\dot{\phi}_o &= \dot{\psi} \\
\left.\begin{aligned} \psi_o &= \frac{\pi}{12} \text{ rad} \\ \phi_o &= 0 \text{ rad} \end{aligned}\right\} \theta_o &= \frac{\pi}{12} \text{ rad} \\
r &= 5.5 \text{ m} \\
R_o &= r + 12 \text{ m} \\
a &= 0.275 \times r \text{ m} \\
m &= 1{,}000 \text{ kg} \\
A &= 0.086 \text{ m}^2
\end{aligned}
\qquad , \qquad (18)
$$

yielded the results shown in Figure 10.

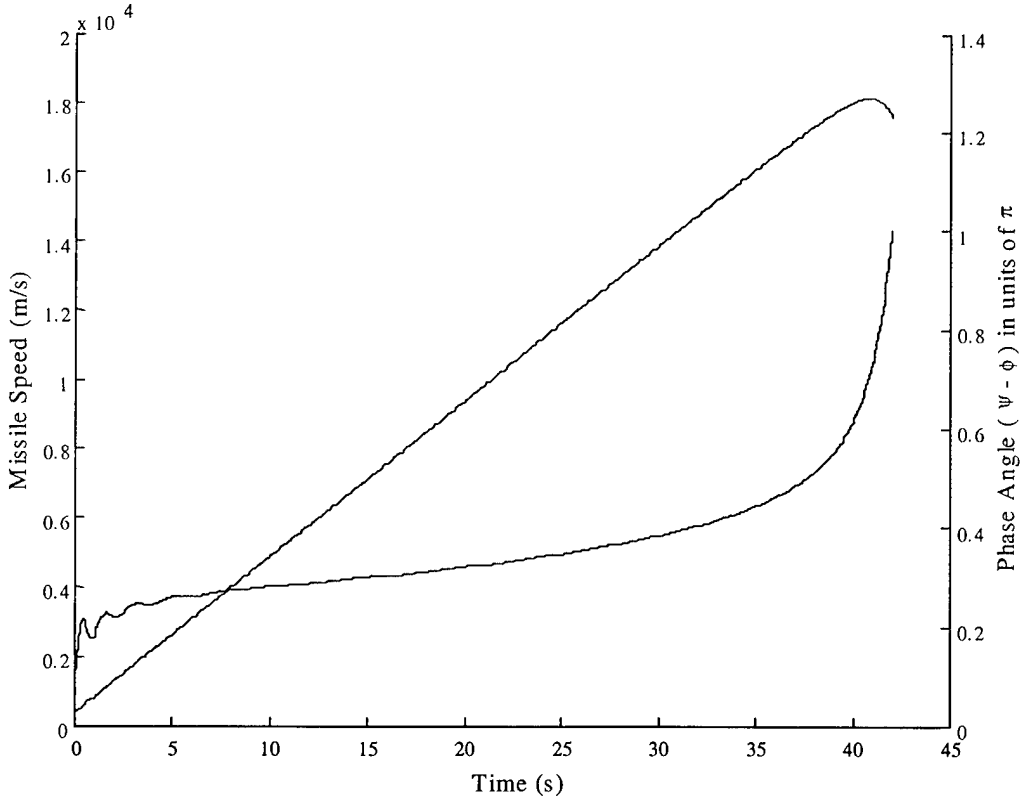

Figure 10. Velocity and Phase Angle vs. Time, Based Upon the Simulink Solution of Equation 11 for the Conditions of Equation 18.

Several features can be pointed to in Figure 10. For instance, it appears that the solution for the missile's speed (Equation 17) increases in a near-linear fashion, almost independent of the phase angle, $\theta = \psi - \phi$, until such a time (~40 s) that the phase angle exceeds some critical value, here ~0.6 π rad (~108°), above which it grows rapidly while the speed declines. Since $\dot{\psi}$ is a constant, in order for the phase angle to change dramatically, $\dot{\phi}$ must change dramatically, as is shown to be the case in Figure 11. There, it can be seen that after initial fluctuations damp out, $\dot{\phi}$ stays fairly steady (about 0.5 rad/s above that of $\dot{\psi}$) until ~40 s, then it declines rapidly. Presumably, it is the decline in $\dot{\phi}$ (though still positive), along with the fact that $\cos\theta$ becomes negative, that explains why the speed in Equation 17 diminishes at around 40 s. However, the decline in speed in this case occurs well above the sought after launch velocity of 8 km/s, which occurs at ~17 s for this particular set of slingatron parameters.

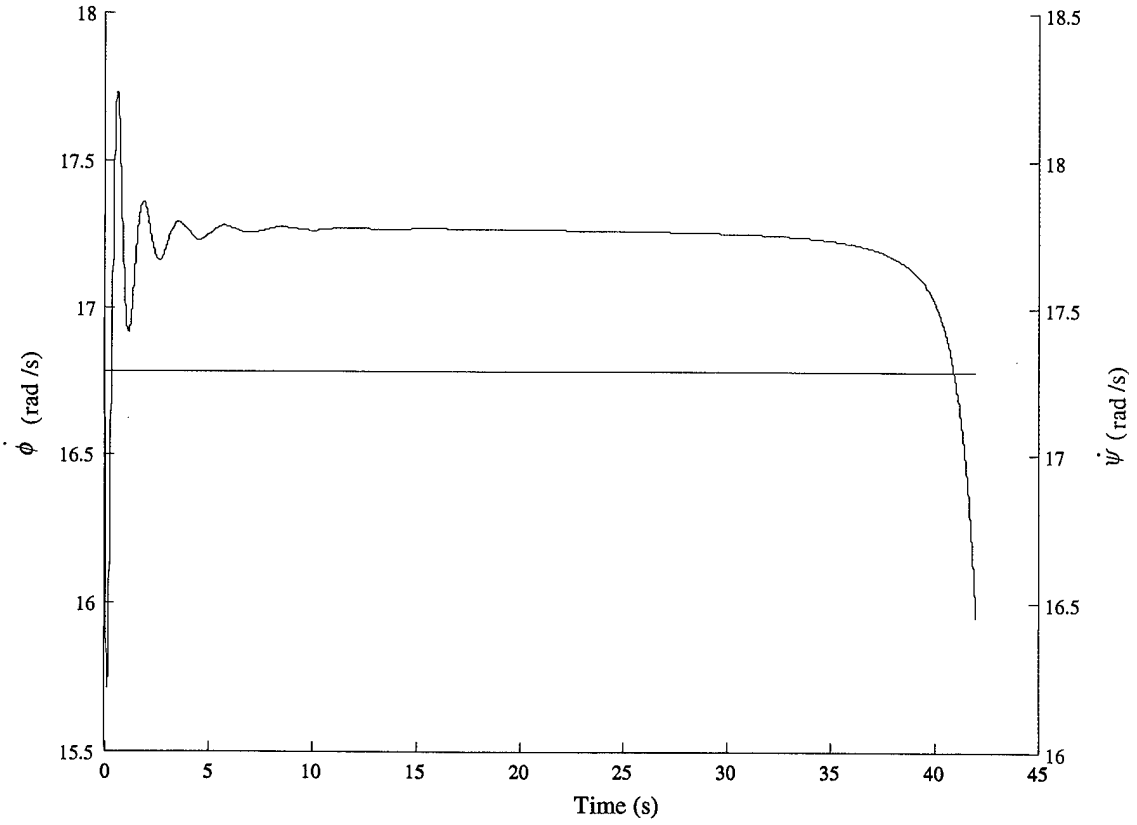

Figure 11. Angular Rates vs. Time, Based Upon the Simulink Solution of Equation 11 for the Conditions of Equation 18.

Figure 12 plots the acceleration of the projectile in the tangent and normal direction to the spiral (corresponding to the same solution as that of Figures 10 and 11). Although it is the nonzero tangential acceleration that gives rise to the speed increase in Figure 10, it can be seen that this component is minor in comparison to the acceleration that the projectile undergoes in the direction normal to the track (e.g., ~100 g's vs. ~14,000 g's at the time the projectile reaches 8 km/s).

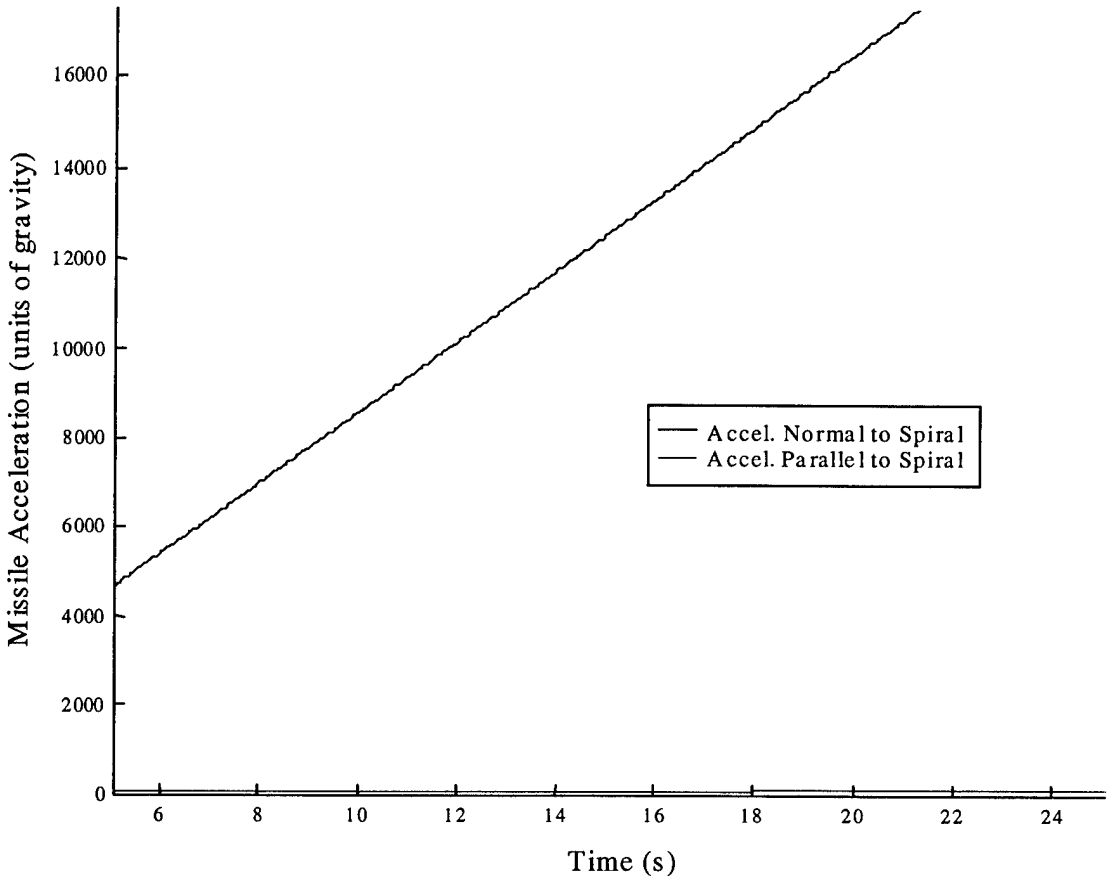

Figure 12. Acceleration vs. Time, Based Upon the Simulink Solution of Equation 11 for the Conditions of Equation 18.

The high acceleration of the projectile normal to the track requires a large normal force, creating a substantial wall pressure, displayed in Figure 13. In practice, a track formed from steel pipe would require a considerable wall thickness to accommodate the level of pressure indicated in Figure 13. A finite element model was formulated to analyze the problem. In particular, a time varying pressure load was swept across one side (180°) of the inner surface of

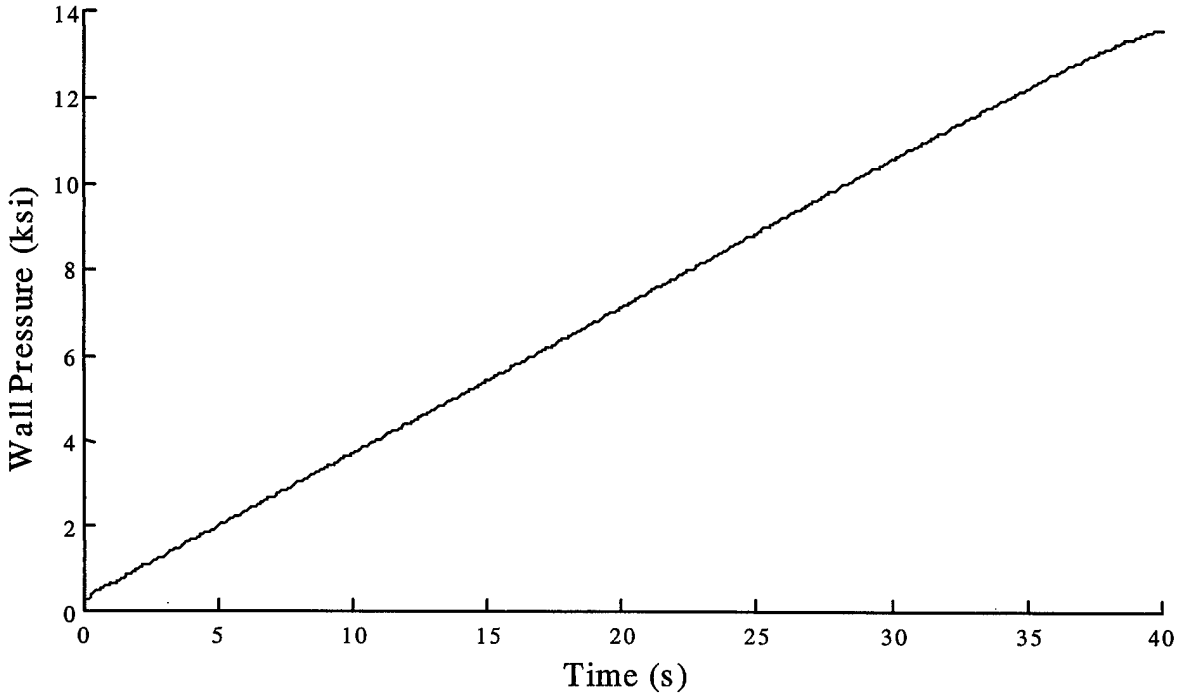

Figure 13. Projectile-Track Interface Pressure vs. Time, Based Upon the Simulink Solution of Equation 11 for the Conditions of Equation 18.

a steel tube, Figure 14, assumed to be hinged at both ends. A plot of the peak hoop (circumferential) stress in the tube as a function of wall thickness is also shown in Figure 14, for various pipe thicknesses. For example, if a wall pressure of 10 ksi were required to change the projectile's direction in the spiral track, then it would generate a peak inner surface hoop stress of ~6–7 ksi in a 2-in-thick wall. If the wall were twice as thick, 4 in, the interaction would produce roughly half the peak hoop stress, ~3–4 ksi. (For reference, 70 ksi is considered a safe hoop-stress level in gun barrel steels.) In the pressure vessel industry, a simple rule of thumb for gauging wall thickness is (Dorf 1996)

$$\text{Wall Thickness (in)} = \frac{\text{Applied Normal Pressure (psi)} \times \text{Inside Cylinder Radius (in)}}{\text{Allowable Stress (psi)} - 0.6 \times \text{Applied Normal Pressure (psi)}} \quad . \quad (19)$$

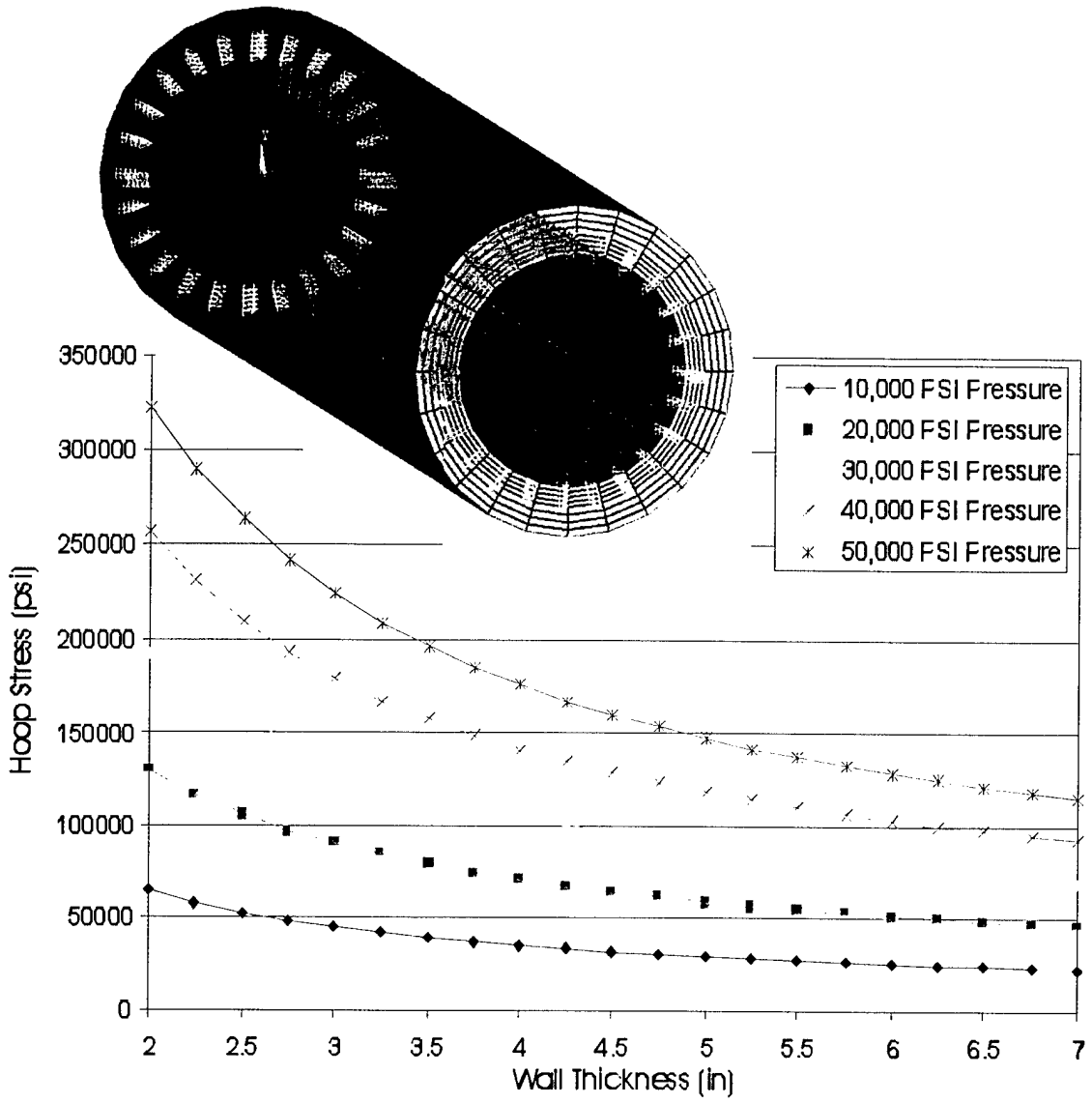

Figure 14. Peak Inner Surface Hoop Stress vs. Wall Thickness for Various Semi-Circular, Inner Wall Pressure Loadings in an AISI 4340 Steel Pipe.

Figure 15 shows the cumulative arc (track) length vs. time for the same Simulink solution as that of Figures 9–13. At 17 s (~8 km/s), the spiral length is ~ 43 mi. An estimate for the weight of such a slingatron track can be made. Assume the track is made from steel that can safely tolerate a hoop stress of 70 ksi. From *A* in Equation 18, the inner radius of the track is 12.5 in (0.32 m) and the wall pressure vs. track length, rather than time (Figure 13), can easily be computed. With this information, Equation 19 provides the wall thickness vs. arc length, from which it can be determined that 43 mi of track would weigh ~17,000,000 lb, or 8,500 tons.

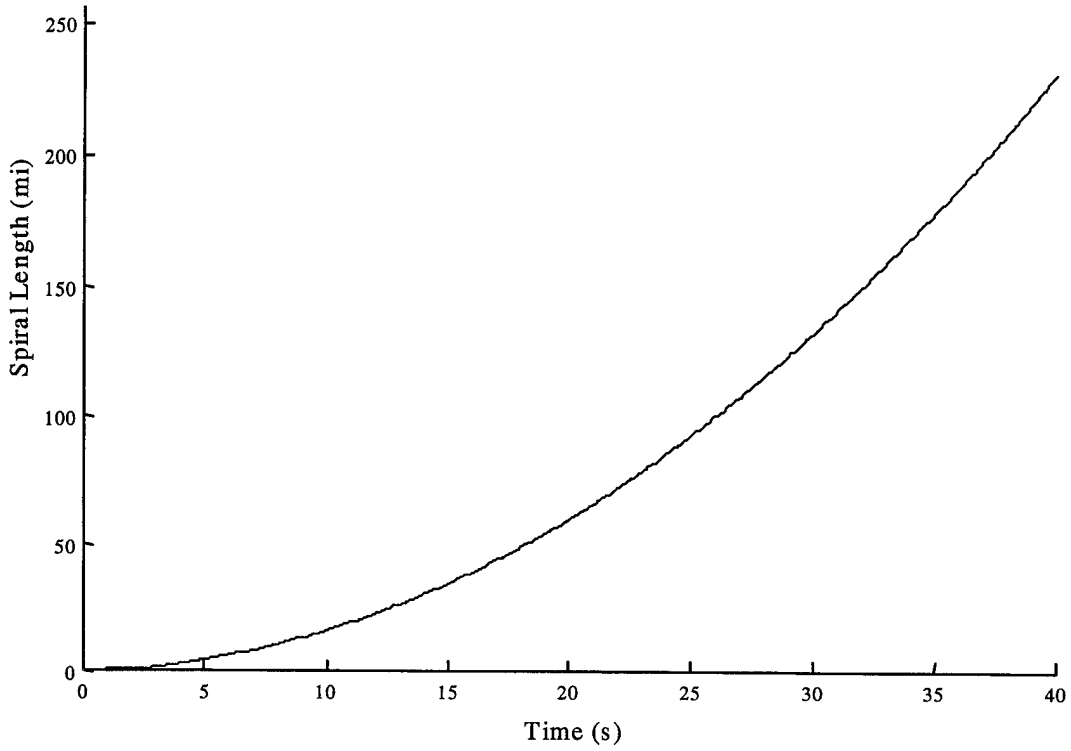

Figure 15. Track Length vs. Time, Based Upon the Simulink Solution of Equation 11 for the Conditions of Equation 18.

Upon closer inspection, it was noticed that within the 90 parameter sets that yielded successful solutions, variation in θ_o and R_o did not strongly affect the outcome. To illustrate this, Figure 16 plots solutions derived from the following subset of Equation 16

$$\dot{\psi} = \frac{11\pi}{2} \text{ rad/s} \quad ; \quad \dot{\phi}_o = \dot{\psi} \quad ; \quad r = 5.5 \text{ m} \quad ; \quad R_o = r+12 \text{ m}$$

$$a = 0.275 \times r \text{ m} \quad ; \quad m = 1{,}000 \text{ kg} \quad ; \quad A = 0.086 \text{ m}^2 \qquad . \quad (20)$$

$$\left.\begin{array}{l} \psi_o = \frac{\pi}{8}, \frac{\pi}{10}, \frac{\pi}{12} \text{ rad} \\ \phi_o = 0 \text{ rad} \end{array}\right\} \theta_o = \frac{\pi}{8}, \frac{\pi}{10}, \frac{\pi}{12} \text{ rad}$$

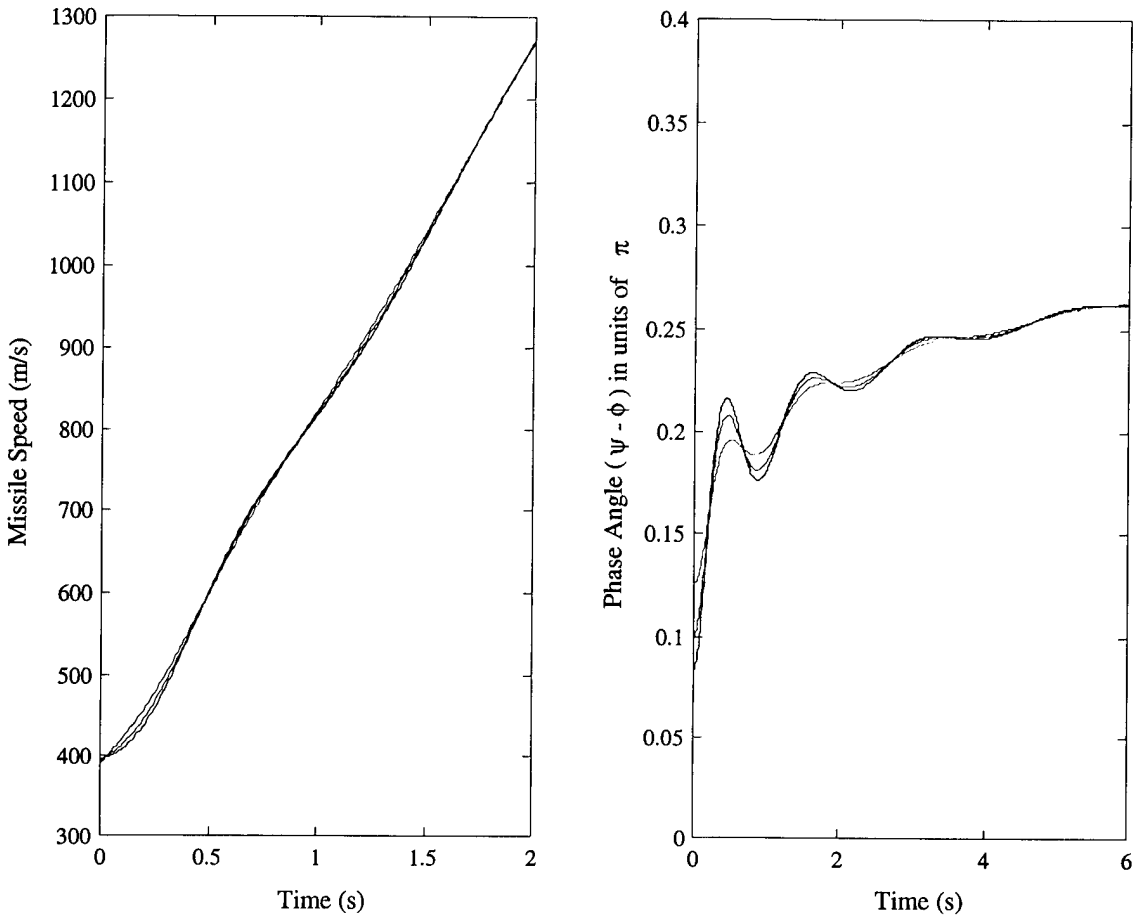

Figure 16. Speed and Phase Angle vs. Time, Based Upon the Simulink Solution of Equation 11 for the Conditions of Equation 20.

As indicated, these three cases differ from each other only by the initial phase angle θ_o. It can be seen from Figure 16, variation in the phase angle dampens out, as did its affect on the solution for the projectile's speed. Likewise, though not plotted here, variation in phase angle did not produce significant changes in the total track length, nor did it noticeably affect the plot of wall pressure vs. time.

A similar result was found to hold for variation in R_o; to demonstrate, consider the following three parameter sets (another subset of Equation 16):

$$\dot{\psi} = \frac{11\pi}{2} \text{ rad/s} \quad ; \quad \dot{\phi}_o = \dot{\psi} \quad ; \quad r = 5.5 \text{ m} \quad ; \quad \theta_o = \frac{\pi}{12} \text{ rad}$$

$$a = 0.275 \times r \text{ m} \quad ; \quad m = 1{,}000 \text{ kg} \quad ; \quad A = 0.086 \text{ m}^2 \quad , \quad (21)$$

$$R_o = r+8,\ r+10,\ r+12 \quad \text{m}$$

where R_o is the only parameter that varies. Solving Equation 11 for each of the three parameter sets in Equation 21 yielded the results shown in Figure 17 for speed and total track length vs. time. Note there is very little difference in the results. This is also the case if wall pressure were plotted vs. time.

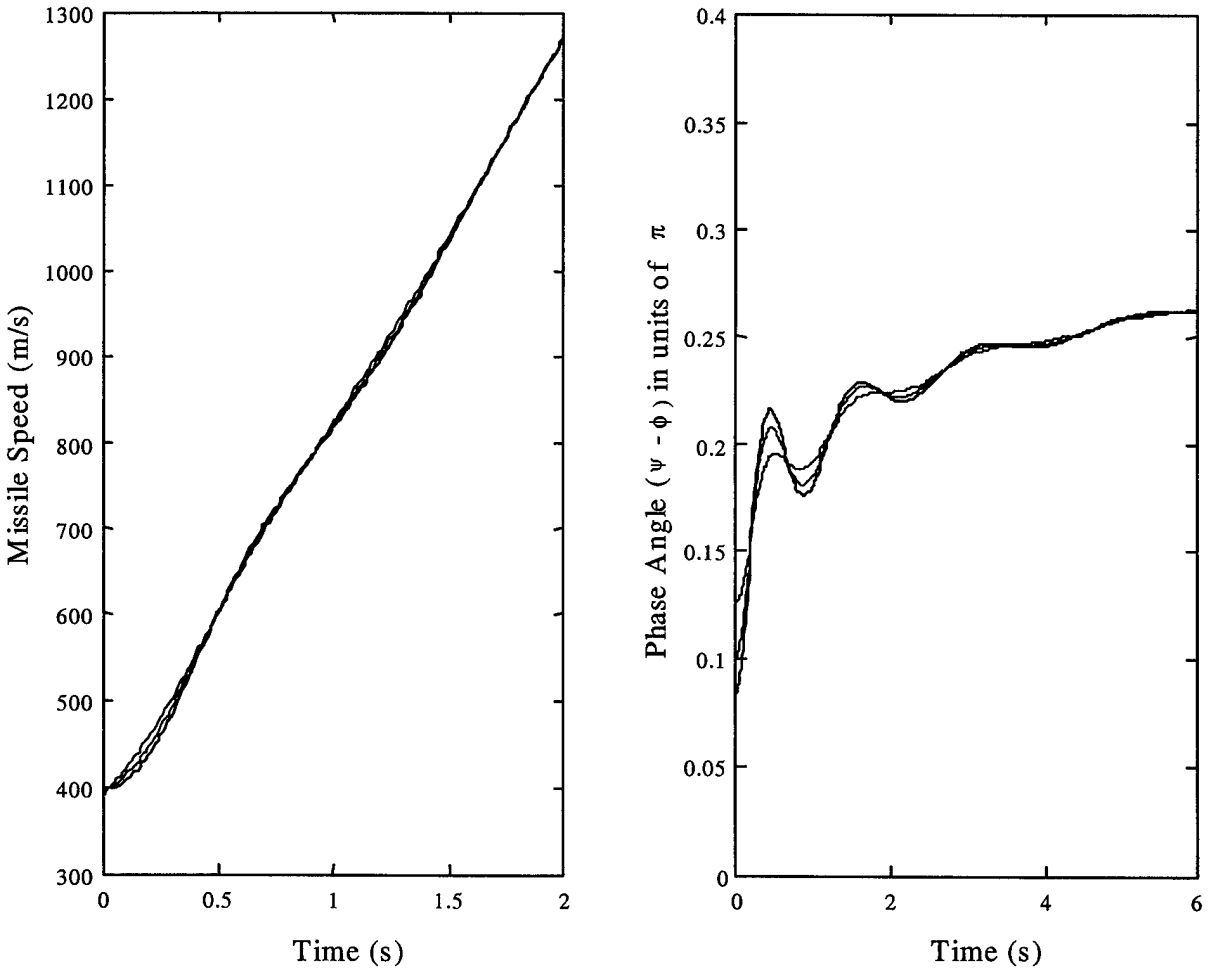

Figure 17. Speed and Track Length vs. Time, Based Upon the Simulink Solution of Equation 11 for the Conditions of Equation 21.

In summary, of the 243 parameter sets specified in Equation 16, only 90 yielded a solution that produced a projectile speed of 8 km/s (or more). Of these 90, only 10 solutions had values for the total track length and wall pressure that were significantly different from each other. Conversely, of the 90 solutions, there was a subset of 10 that yielded significantly different values for the track length and wall pressure; for each of these 10, there were 9 variations in either θ_o or R_o that only slightly perturbed the length and pressure profiles.

In addition to track length and wall pressure, another factor that must be considered in evaluating a practical slingatron design would be the speed at which the spiral track gyrates. For instance, the higher the frame speed, the more energy is expended doing work against air resistance/drag. Furthermore, the higher the structural speed, the higher the loads on moving parts (e.g., bearings), and the more wear and maintenance that can be expected. Figure 18 plots the frame speed vs. wall pressure and track length for the 90 successful launch solutions of Equation 11. The inset plot shows the 10 most unique solutions, demonstrating that variation in θ_o and R_o is not needed to capture the gross range of solutions.

The most desirable solution is the one that has a low track speed, low wall pressure, and short track length; not surprisingly, concurrent minimums in these three parameters appear unachievable. Thus, a compromise has to be made—two of the three desirable traits must be favored at the expense of the third, or less than minimum values must be accepted for all three factors. For example, from Figure 18, if a maximum wall pressure at projectile exit of 6 ksi could be tolerated, then a minimum spiral length of 43 mi, gyrating at a minimum circular speed of 95 m/s could be achieved. On the other hand, if the maximum wall pressure was set at 5 ksi, it would necessitate a minimal spiral length of 66 mi with a frame speed of 78 m/s. Also shown in Figure 18 are three solutions where the pressure is 5 ksi and the frame speed is 78 m/s, but the track lengths are vastly different, at 66 mi, 80 mi, and 102 mi, respectively. Although these three designs accomplish the same effect (e.g., launching the projectile into space at 8 km/s), the difference in their costs (one being 40% shorter than the other) would be tremendous, thus proving the potential benefit of this type of parametric analysis.

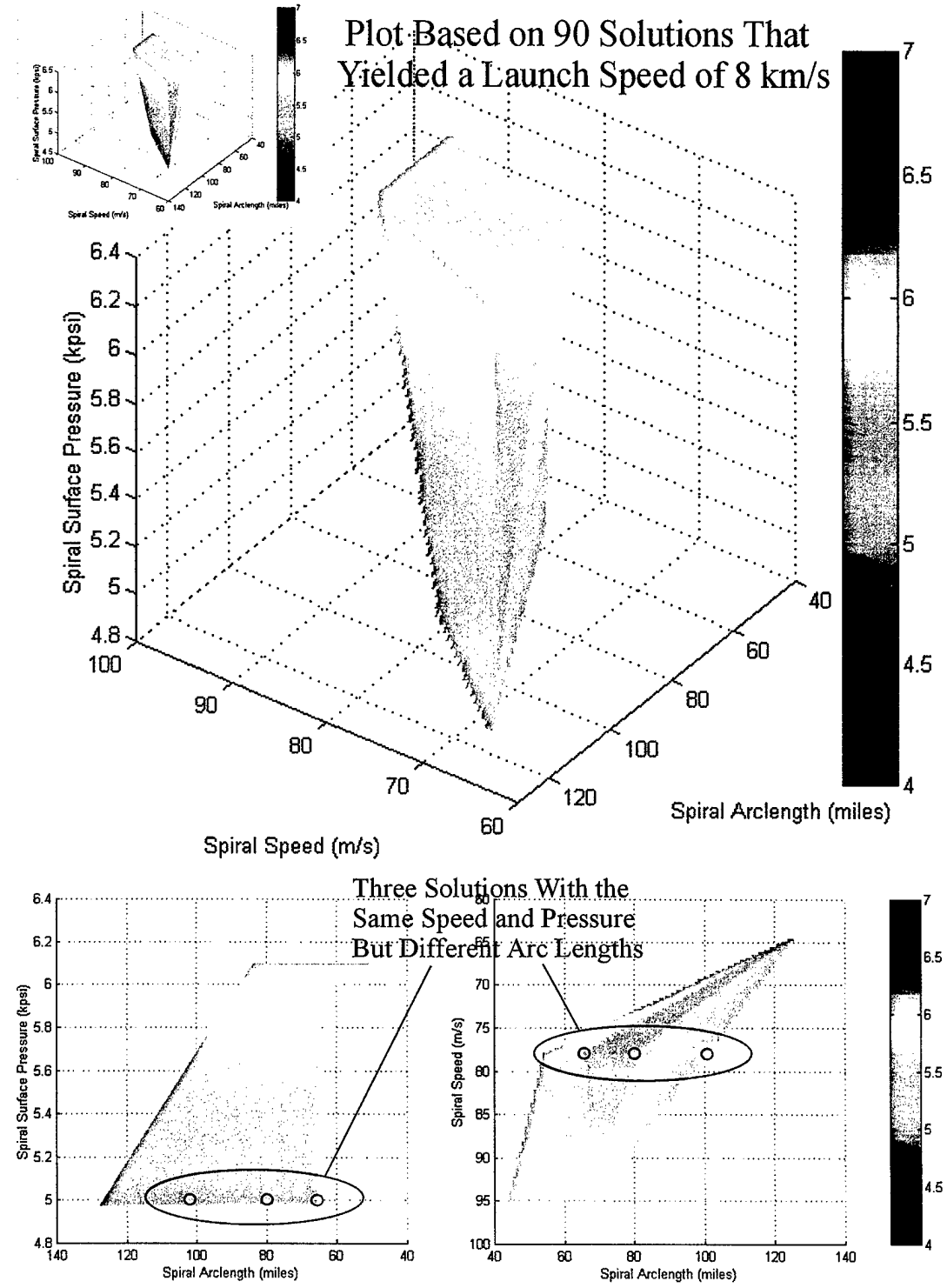

Figure 18. Wall Pressure vs. Spiral Speed vs. Spiral Track Length, Based Upon the Simulink Solution of Equation 11 for the Conditions of Equation 16.

The relatively small range of parameters specified in Equation 16 has been used to demonstrate (via Figures 10–18) the methodology by which Simulink can be utilized to search for favorable solutions to the problem of a slingatron-based earth-to-space projectile launch, from an engineeringly practical vantage point.

Although Figure 18 shows a solution surface, the range of parameters upon which it was derived, viz., Equation 16 (with its 243 possibilities), is not all-inclusive. Are there other parameter sets that might produce even better (easier to produce and maintain) solutions/designs? To answer this question, a broader range of parameters needs to be examined. In order to explore the widest possible range of solutions with the minimum computer time and resources, it is sensible to distribute the collection of parameters in accordance with their degree of influence on the solution. As indicated by the likeness of the 10-solution subset to the full 90-solution assembly in Figure 18, variation in the parameters θ_o and R_o does not produce significantly different results. Therefore, it makes sense to narrow the range of these two parameters and widen the range for the remaining three, viz., the gyration speed parameter, $\dot{\psi}$, the gyration radius, r, and the parameter governing the tightness of the spiral, a. Accordingly, the following 18,375 parameter sets were examined and (as will be shown) found to yield a range of solutions that liberally bounded the region of practical interest.

$$
\begin{aligned}
&\dot{\psi} = \frac{\pi}{2}\left(2n_1 - 1\right)\text{rad/s} \;;\; \text{for}\;\; n_1 = 1{:}35 \\
&\dot{\phi}_o = \dot{\psi} \\
&\left.\begin{aligned}\psi_o &= \frac{\pi}{40}\,\text{rad} \\ \phi_o &= 0\;\text{rad}\end{aligned}\right\} \theta_o = \frac{\pi}{40}\;\text{rad} \\
&r = n_2 - 0.5\;\text{m} \;;\; \text{for}\;\; n_2 = 1{:}35 \\
&R_o = r+8,\; r+10,\; r+12\;\;\text{m} \\
&a = \left(n_3 - 0.5\right)\times 0.05 \times r\;\;\text{m} \;;\; \text{for}\;\; n_3 = 1{:}15 \\
&m = 1{,}000\;\;\text{kg} \\
&A = 0.086\;\;\text{m}^2
\end{aligned}
\qquad , \qquad (22)
$$

Out of the 18,375 different combinations of parameters, there were 16,178 successful solutions (of Equation 11 for $\phi[t]$) that yielded a projectile speed (Equation 17) of at least 8 km/s. Figure 19 is the counterpart of Figure 18, displaying all 16,178 solutions.

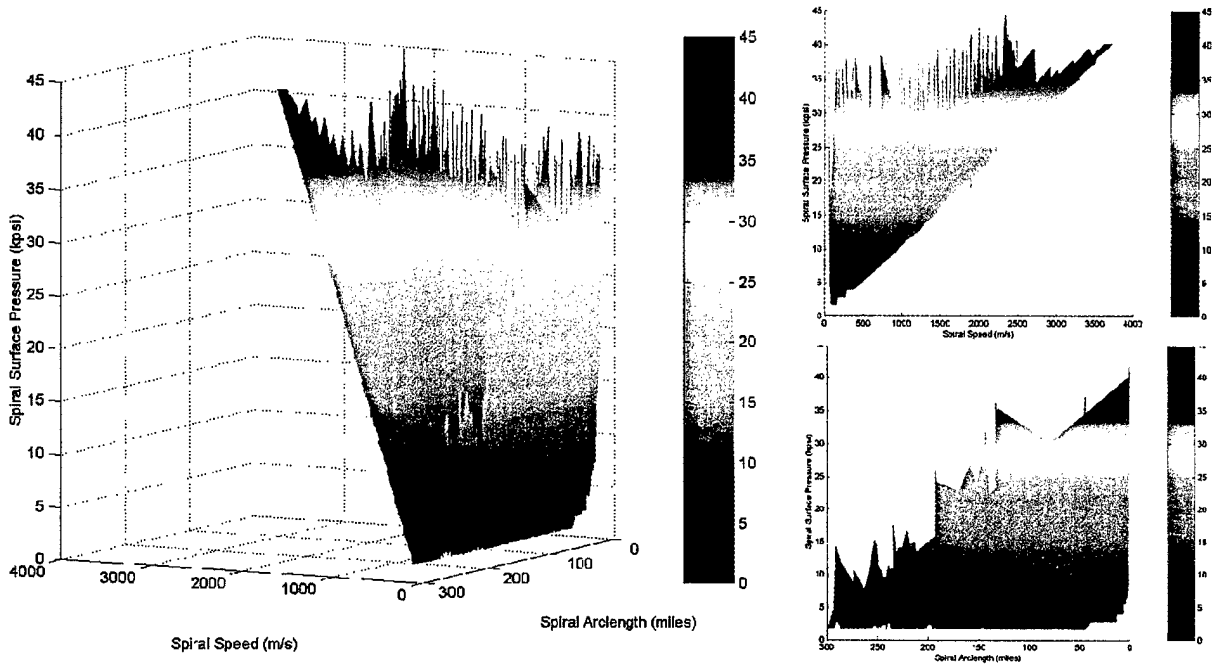

Figure 19. Wall Pressure vs. Spiral Speed vs. Spiral Track Length, Based Upon the Simulink Solution of Equation 11 for the Conditions of Equation 22.

Clearly, a structural speed that is greater than the speed of sound (~335 m/s) is impractical, neglecting these cases would eliminate the majority of the solutions indicated in Figure 19. A more reasonable speed might be several hundred meters per second slower. Searching the solution set, Figure 20 shows a subset plot of 600 solutions, where the structural speed of the track was < 140 m/s, and the track length is < ~100 mi.

At the upper speed end in this subset is a solution (n_1 = 2, n_2 = 30, n_3 = 13) where the structure is moving at 139 m/s (313 mph), the peak wall pressure is below 2 ksi, and the track length is a relatively moderate 54 mi. Based on the same approach used to determine the 8,500-ton track weight in the previous (95-m/s, 6-ksi, 43-mi) example, this 54-mi, (presumed) upper-speed-limit track would weigh a relatively low 2,700 tons.

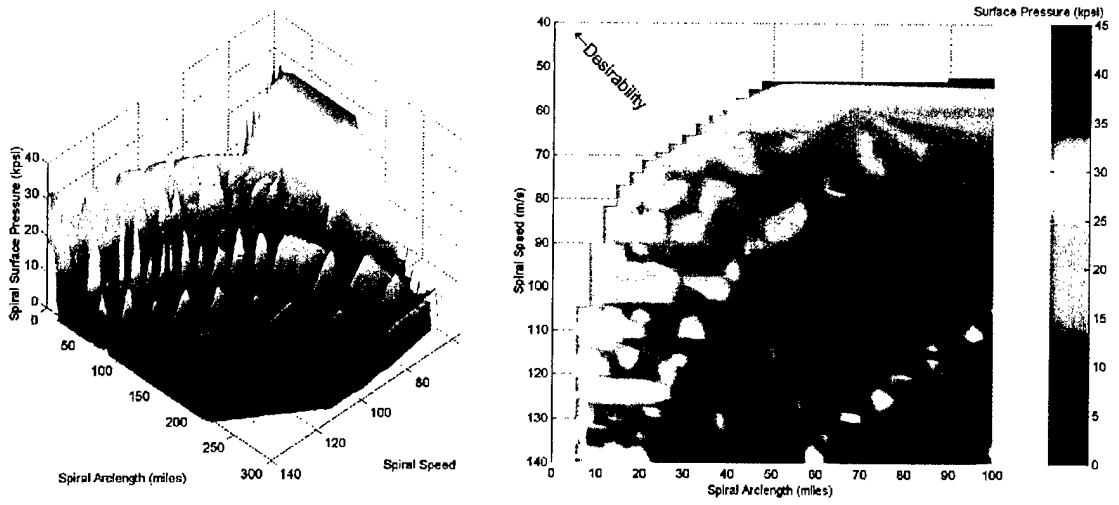

Figure 20. Wall Pressure vs. Spiral Speed vs. Spiral Track Length, Based Upon the Simulink Solution of Equation 11 for the Conditions of Equation 22.

At the low speed end, a solution exists ($n_1 = 34$, $n_2 = 1$, $n_3 = 2$) where the track motion is slowed down to 53 m/s; the track length remains in the middle ground at 48 mi, but the wall pressure peaks at 37 ksi. The estimated weight of this lower-speed-limit track is relatively high at 107,000 tons.

A more all-around-moderate solution ($n_1 = 7$, $n_2 = 4$, $n_3 = 6$) has the track motion at 72 m/s, the wall pressure at 7 ksi, and the track length again in the mid-range at 50 mi. The estimated weight of this track would be 12,200 tons.

Perhaps the best solution compromise for structural speed, peak wall pressure, length, and weight is one ($n_1 = 10$, $n_2 = 3$, $n_3 = 7$) that produces mid-range values for the frame speed at 75 m/s, wall pressure at 11 ksi, weight at 10,500 tons, and a low-end track length at 28 mi. Such a structure would fit within a 550-m-diameter circle, an artistic rendering of which is shown in Figure 21.* (For reference, this slingatron would be the weight-motion equivalent of two fully loaded medium-sized river barges, each circling at ~5 hz around a respective radius of ~8 ft, or 170 mph.)

* Rendering provided by Mark L. Kregel.

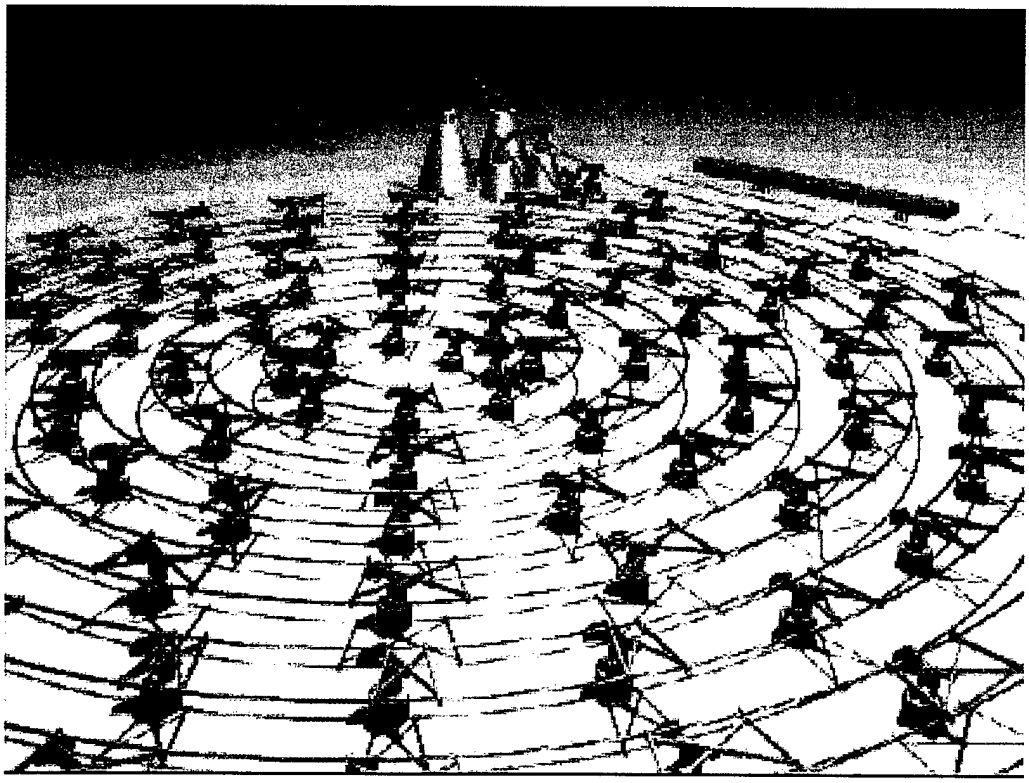

Figure 21. A Conceptual Sketch of an Earth-to-Space Slingatron Launcher.

Although the evidence is anecdotal, the values for n_1, n_2, and n_3 in the four practical-solution examples described previously and tabulated in Table 1 (spanning the high, moderate, and low frame speed regimes) serve to illustrate that the range of n_1 and n_2, from 1–35, and n_3, from 1–15, was broad enough to capture the majority, if not all, of the most practical slingatron designs.

Table 1. Examples of the "Most Practical/Optimum" Slingatron Track Designs

Minimum Values	Structural Speed (m/s)	Wall Pressure (ksi)	Track Length (miles)	Weight (U.S. tons)
A	139	2	54	2,700
B	53	37	48	107,000
C	72	7	50	12,200
D	75	11	28	10,500

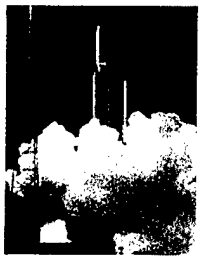

Titan IV Rocket —340-380 tons

International Space Station —520 tons

500-ft Fully Loaded Cargo Ship—8,000 tons

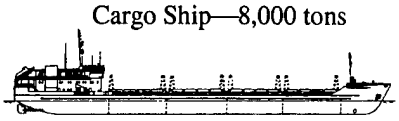

Large Steel River Bridge—10,000 tons

1000-ft Fully Loaded Aircraft Carrier — 80-100,000 tons

Golden Gate Bay Bridge — 200,000 tons

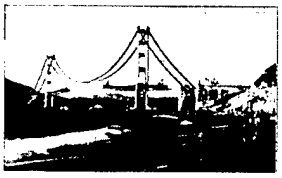

6. Summary

This report provides a physical explanation of the mechanism by which the mechanical device referred to as a slingatron, akin to a Hula-Hoop, can be used to launch a projectile. Furthermore, using the software program called Simulink (a complementary program to MATLAB) the nonlinear differential equation of motion for a spiral slingatron design was solved for a large range of input parameters. These solutions were sorted based upon whether or not the slingatron design could accelerate a 1000-kg, 0.64-m-diameter projectile to at least 8 km/s (assumed to be a sufficient speed to place such a payload into space). Finally, the most physically reasonably of these successful solutions were down selected. For example, a spiral track 28 mi long, weighing 10,500 tons, and having a structural speed of ~170 mph could be used to launch such a projectile into space. With the type of information provided in this study (viz., structural speed, wall pressure, and track length), a more detailed track design analysis could begin, leading to (among other things) a sound total dollar (or per-payload-pound) cost estimate for a slingatron-based, earth-to-space launch system.

6. References

Dorf, R. C. *The Engineering Handbook.* Boca Raton, FL: CRC Press Inc, p. 85, 1996.

Liepman, H. W., and A Roshko. *Elements of Gasdynamics.* New York: John Wiley & Sons, p. 64, 1957.

MATLAB. *MATLAB Notebook User's Guide.* Version 5, The Mathworks, Inc., Natick, MA, 1998.

Tidman, D. A., R. L. Burton, D. S. Jenkins, and F. D. Witherspoon. "Sling Launch of Materials into Space." *Proceedings of 12th SSI/Princeton Conference on Space Manufacturing*, ed. By B. Faughnan, Space Studies Institute, Princeton, NJ, pp. 59–70, May 1995.

Tidman, D. A. "Sling Launch of a Mass Using Superconducting Levitation." *IEEE Transactions on Magnetics,* vol. 32, no. 1, pp. 240–247, January 1996.

Tidman, D. A. "Slingatron Mass Launchers." *Journal of Propulsion and Power*, vol. 14, no. 4, pp. 537–544, July–August 1998.

Tidman, D. A., and J. R. Greig. "Slingatron Engineering and Early Experiments." *Proceedings of the 14th SSI/Princeton Conference on Space Manufacturing.* ed. by B. Faughnan, Space Studies Institute, Princeton, NJ, pp. 306–312, May 1999.

Tidman, D. A. "The Spiral Slingatron Mass Launcher." *Proceedings of the 10th U.S. Army Gun Dynamics Symposium*, Austin, TX, April 2001.

INTENTIONALLY LEFT BLANK.

NO. OF COPIES	ORGANIZATION
2	DEFENSE TECHNICAL INFORMATION CENTER DTIC OCA 8725 JOHN J KINGMAN RD STE 0944 FT BELVOIR VA 22060-6218
1	HQDA DAMO FDT 400 ARMY PENTAGON WASHINGTON DC 20310-0460
1	OSD OUSD(A&T)/ODDR&E(R) DR R J TREW 3800 DEFENSE PENTAGON WASHINGTON DC 20301-3800
1	COMMANDING GENERAL US ARMY MATERIEL CMD AMCRDA TF 5001 EISENHOWER AVE ALEXANDRIA VA 22333-0001
1	INST FOR ADVNCD TCHNLGY THE UNIV OF TEXAS AT AUSTIN 3925 W BRAKER LN STE 400 AUSTIN TX 78759-5316
1	DARPA SPECIAL PROJECTS OFFICE J CARLINI 3701 N FAIRFAX DR ARLINGTON VA 22203-1714
1	US MILITARY ACADEMY MATH SCI CTR EXCELLENCE MADN MATH MAJ HUBER THAYER HALL WEST POINT NY 10996-1786
1	DIRECTOR US ARMY RESEARCH LAB AMSRL D DR D SMITH 2800 POWDER MILL RD ADELPHI MD 20783-1197

NO. OF COPIES	ORGANIZATION
1	DIRECTOR US ARMY RESEARCH LAB AMSRL CI AI R 2800 POWDER MILL RD ADELPHI MD 20783-1197
3	DIRECTOR US ARMY RESEARCH LAB AMSRL CI LL 2800 POWDER MILL RD ADELPHI MD 20783-1197
3	DIRECTOR US ARMY RESEARCH LAB AMSRL CI IS T 2800 POWDER MILL RD ADELPHI MD 20783-1197
	ABERDEEN PROVING GROUND
2	DIR USARL AMSRL CI LP (BLDG 305)

NO. OF COPIES	ORGANIZATION
1	NASA LANGLEY RSRCH CENTER D BUSHNELL MS 10 HAMPTON VA 23681-2189
3	NASA HEADQUARTERS L GUERRA WASHINGTON DC 20546-0001
3	NASA MARSHALL SPACE FLIGHT CTR J JONES B 4203 RM 2131 HUNTSVILLE AL 35812
	ABERDEEN PROVING GROUND
9	DIR USARL AMSRL WM A HORST E SCHMIDT AMSRL WM BD P PLOSTINS J NEWILL G COOPER M BUNDY (3 CPS) AMSRL WM BE M NUSCA

USER EVALUATION SHEET/CHANGE OF ADDRESS

This Laboratory undertakes a continuing effort to improve the quality of the reports it publishes. Your comments/answers to the items/questions below will aid us in our efforts.

1. ARL Report Number/Author ARL-TR-2555 (Bundy) Date of Report August 2001

2. Date Report Received _____

3. Does this report satisfy a need? (Comment on purpose, related project, or other area of interest for which the report will be used.) _____

4. Specifically, how is the report being used? (Information source, design data, procedure, source of ideas, etc.) _____

5. Has the information in this report led to any quantitative savings as far as man-hours or dollars saved, operating costs avoided, or efficiencies achieved, etc? If so, please elaborate. _____

6. General Comments. What do you think should be changed to improve future reports? (Indicate changes to organization, technical content, format, etc.) _____

CURRENT ADDRESS

_____
Organization

_____
Name E-mail Name

_____
Street or P.O. Box No.

_____
City, State, Zip Code

7. If indicating a Change of Address or Address Correction, please provide the Current or Correct address above and the Old or Incorrect address below.

OLD ADDRESS

_____
Organization

_____
Name

_____
Street or P.O. Box No.

_____
City, State, Zip Code

(Remove this sheet, fold as indicated, tape closed, and mail.)

(DO NOT STAPLE)